Chemistry–A European Journal
Research Article
doi.org/10.1002/chem.202202330
Chemistry Europe
European Chemical Societies Publishing
www.chemeurj.org

Room-Temperature-Observable Interconversion Between Si(IV) and Si(II) via Reversible Intramolecular Insertion Into an Aromatic C–C Bond

Teresa Eisner,[a] Arseni Kostenko,[a] Franziska Hanusch,[a] and Shigeyoshi Inoue*[a]

Abstract: An easily isolable silacycloheptatriene (silepin) **1 b** was synthesized from the reaction of a *N*-heterocyclic imino (IPrN) substituted tribromosilane IPrNSiBr$_3$ with the sterically congested bis(trimethylsilyl)triisopropylsilyl silanide KSi(TMS)$_2$Si(^{i}Pr)$_3$ (BTTPS). In solution, the Si(IV) silepin **1 b** is in a thermodynamic equilibrium with the acyclic Si(II) silylene **1 a**. The relative concentration of the Si(II) or Si(IV) isomers can be controlled by temperature variation and observed by variable temperature NMR and UV/Vis spectroscopy. DFT calculations show a small reaction barrier for the Si(II)⇌Si(IV) interconversion and a small energy gap between the Si(II) and Si(IV) species. The reactivity of **1 a/b** is demonstrated on a variety of small molecules.

Introduction

Since the discovery of the first Si(II) compound, i.e. the decamethylsilicocene (**A**) (Figure 1), by Jutzi in 1989,[1] silylenes [:SiR$_2$] have attracted significant attention due to their ambiphilic nature and many examples have been reported up to date. Silylenes are the heavier analogs of carbenes [:CR$_2$], which can exist in the singlet and the triplet ground state, depending on substituents. In contrast to their lighter congeners, however, silylenes have been primarily reported in the singlet ground state due to the reduced hybridization tendency of silicon.[2]

The frontier molecular orbitals of silylenes are a lone pair with high s-character (HOMO), and a vacant *p*-orbital (LUMO). Such arrangement, in regard to small molecule activation, mimics the frontier *d*-orbitals of transition metals, showing their potential to imitate their reactivity. In general, the properties of such species are highly influenced by the electronic and steric nature of their substituents, as they affect the geometry at the silicon center. Sterically demanding substituents tend to increase the R–Si–R′ angle resulting in a smaller HOMO-LUMO gap and thus leading to increased reactivity.[2–3]

Due to these properties, a variety of oxidative addition reactions (OA) towards small molecules, such as N_2O,[4] ethylene,[5] or CO_2,[6], forming the corresponding Si(IV) compounds, are known. These oxidative addition processes have been in the focus of investigations with the ultimate goal to deploy silicon, the second most abundant element in earth's crust, as a catalytically active element. Despite the extraordinary capabilities of silylenes in small molecule activation, development of silicon based catalytic reactions is an arduous journey due to the inherent proclivity of silicon to be in the +IV oxidation state. The reversible retrieval of Si(II) *via* malleable reductive elimination (RE), representing the second key step to catalytic applications, remains a challenge in silicon chemistry.

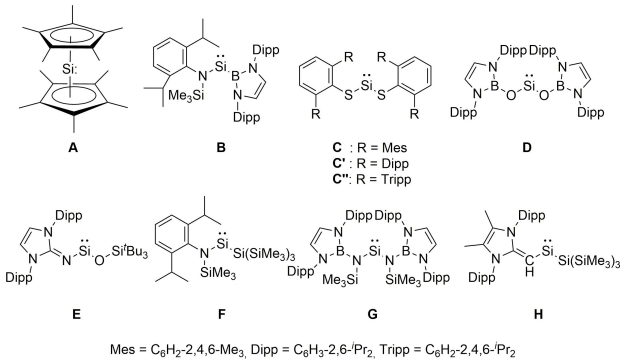

Figure 1. Selected examples of acyclic silylenes.

As Si(II) species are highly reactive, only cyclic or Lewis base-stabilized (three coordinate) silylenes were known up until 2012, when the first acyclic representatives, the (amido)boryl silylene (**B**) and the thiolato-substituted **C**, were published.[3,7]. Up to date, a few additional acyclic examples were reported, all of which rely on sterically encumbered ligands. Compared to their cyclic counterpart, those silylenes possess an enlarged R–Si–R^2 bond angle resulting in elevated reactivity toward small molecules. Other isolated examples include boryloxy- (**D**), siloxy- (**E**), as well as amino- (**F**, **G**) and *N*-heterocyclic olefin- (**F**) ligands, which bridge the gap between the higher reactivity

[a] *T. Eisner, Dr. A. Kostenko, Dr. F. Hanusch, Prof. Dr. S. Inoue*
School of Natural Sciences
Department of Chemistry
WACKER-Institute of Silicon Chemistry and Catalysis Research Centre
Technical University of Munich
Lichtenbergstraße 4, 85748 Garching bei München (Germany)
E-mail: s.inoue@tum.de

Supporting information for this article is available on the WWW under https://doi.org/10.1002/chem.202202330

(due to the increased R–Si–R^2 angle) and a sufficient kinetic and thermodynamic stabilization.

In 2017, our group published an *N*-heterocyclic imine (NHI) substituted silacycloheptatriene (silepin **I**, Figure 2).[13] Variable temperature (VT) UV/Vis studies suggested a reversible formation of the respective silylene **I'** at elevated temperatures, implying a reversible interconversion between the Si(II) and the Si(IV) species. Similar to other acyclic silylenes, compound **I** is capable to selectively react with small molecules such as H_2, ethylene, CO_2, and N_2O[2] under mild conditions, which is possible due to a Si(IV)⇌Si(II) equilibrium. Within the same year the related compound **J**, which is substituted with a supersilyl ($Si(^tBu)_3$) ligand instead of the previously used hypersilyl ligand ($Si(TMS)_3$), was reported.[4b] The silepin shows comparable reactivity as compound **I** and other silylene species. Thus, compounds **I** and **J** can be described as "masked" silylenes.

The insertion of a silylene into an aromatic C–C bond is an uncommon reactivity, with **I** and **J** being among the rare examples. Previously, the synthesis of silepins could be achieved *via* a variety of routes, for example by a double ring-opening reaction of a cyclopropenone with a tetramethylsilole dianion reported by West.[14] Older synthesis routes usually include Si(IV) precursors like dichlorosilanes[15] and 1,2-dimethoxy disilanes[16] instead of low valent silicon species. Few examples of cyclic silylenes, such as a cyclic alkyl amino silylene (CAASi) and a cyclic dialkyl silylene, are known to insert into C–C bonds of aromatic compounds, such as benzene (**K, L**), naphthalene and azulenes.[17] Regarding acyclic silylenes, only three additional examples are known. The first one being the disilene Tbt(Mes)Si=Si(Mes)Tbt published by Okazaki, which dissociates to the respective silylene *via* thermal Si–Si bond cleavage and is thereby able to insert into an aromatic bond of benzene (**M**) or naphthalene.[18] Another example by Cui shows the intramolecular formation of a boryl-substituted silepin **N**, which can be converted into the respective NHC-stabilized hydrosilylene.[19] The most recent example was published by our group. The siloxy-substituted silepin **O** is a follow-up product of silylene **E** and comparable to **I**, it is able to insert into the Dipp-substituent intramolecularly upon heating.[10] Notably, intermolecular silepin formation reactions usually only proceed through thermal activation or through activation *via* UV light at ≈340 nm while the intramolecular examples (except for the siloxysilylene **O**) occur at room temperature without irradiation. Furthermore, for all the examples, except for **I**, **J** and **N**, no reversibility of the C–C bond insertion process was reported.

In our group, we are interested in investigating facile OA/RE processes involving an active Si(II)/Si(IV) center. Since the reactivity of the compounds **I** and **J** indicate that reversible OA/RE *via* intramolecular C–C bond insertion can be achieved, we aimed to expand our investigations and study the influence of steric and electronic effects on the OA/RE process. Thus, we introduced the sterically more demanding **b**is(**t**rimethylsilyl)**t**ri**i**so**p**ropyl**s**ilyl silanide substituent $-Si(TMS)_2Si(^iPr)_3$ (BTTPS) to the Si center. Herein, we present iminosilepin **1 b** featuring the BTTPS substituent, which exists in a spectroscopically observable thermodynamic equilibrium with the iminosilylene **1 a**. In fact, both species are detectible at room temperature and their relative ratio can be manipulated by alternating temperature, demonstrating the reversible interconversion between Si(IV) and Si(II) in a compliant OA/RE process.

Results and Discussion

Compound **1 a/b** was synthesized similarly to the silepin **I**, previously reported by our group. Thereby, two equivalents of the BTTPS ligand were added to bis(2,6-diisopropylphenyl)imidazoline-2-iminotribromosilane ($IPrNSiBr_3$) at −78 °C in toluene and a color change from orange to intensive green could be observed (Scheme 1). NMR spectroscopic measurement of the crude product mixture shows the formation of a mixture of silylene **1 a** and silepin **1 b** along with the side product $BrSi(TMS)_2Si(^iPr)_3$. The desired products **1 a** and **1 b** can be separated from the side product by crystallization of the silepin **1 b** from a concentrated hexane solution at −35 °C as neon yellow crystals. **1 a/b** can be isolated in 70% yield, which is a major advantage compared to the previously

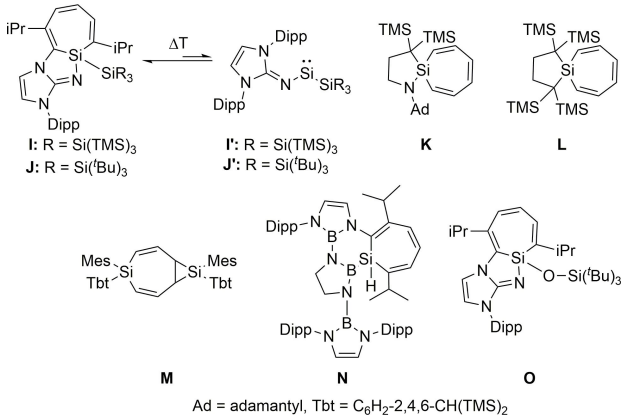

Figure 2. Reported examples of silepins.

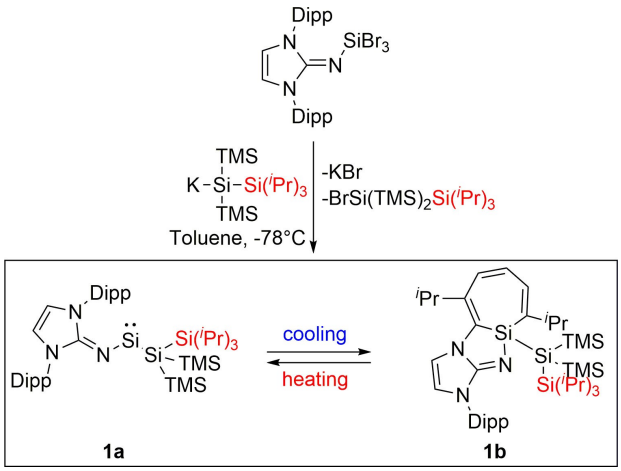

Scheme 1. Synthesis of the silylene **1 a** / silepin **1 b**

reported silepin **I**, where only a 6% yield could be achieved, and the follow-up chemistry relied on freshly prepared batches containing the side product. The high yield and the purity in the case of **1a/b** allows easy access to follow-up reactivity investigations. The molecular structure of silepin **1b** was determined by single crystal X-ray diffraction (SC-XRD, Figure 3). **1b** possesses a tetravalent silicon center inserted into the C16-C21 bond of the Dipp substituent, forming a seven-membered ring with Si–C bond lengths of 1.900 Å and 1.871 Å, respectively. Between the central silicon and the BTTPS substituent the Si1–Si2 bond length is 2.381 Å and between the central silicon center and the nitrogen atom of the NHI substituent (Si1–N1) the atom distance is 1.752 Å. In general, the structural features of **1b** are very similar to those of the previously reported silepin **I**, with only slight elongation of the Si1–Si2 bond (2.342 Å in compound **I**), which is presumably a result of the enhanced steric bulk of the BTTPS ligand. Multiple XRD measurements indicate the sole crystallization of **1b** over **1a**, thus despite multiple different attempts, no crystal structure of the silylene **1a** could be obtained.

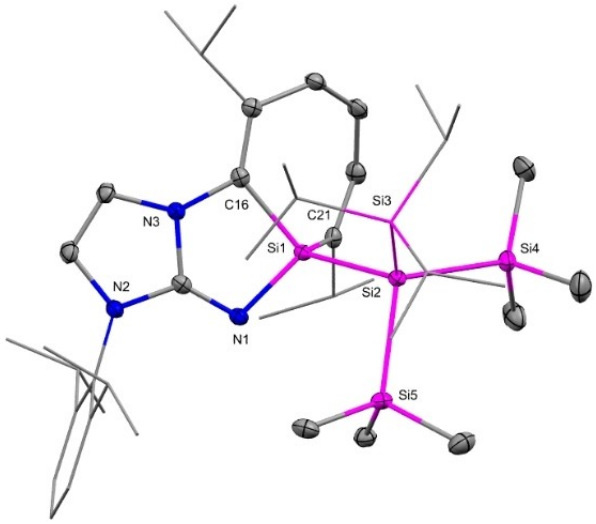

Figure 3. Molecular structure of **1b**. Ellipsoids set at 50% probability; H atoms are omitted for clarity. Selected bond lengths [Å] and angles [°]: Si1-C16 1.900(2), Si1-C21 1.870(2), Si1-N1 1.752(2), Si1-Si2 2.3809(7), C16-Si1-C21 103.33(8), C16-Si1-N1 94.06(7), C21-Si1-Si2 111.47(6).

Room temperature ^{29}Si NMR spectroscopy of a crystalline sample of **1b** in toluene-d8 displays two full sets of signals, confirming the establishment of the **1a/b** equilibrium in solution. Whereas all other **1a/b** signals are in comparable ranges, the central Si signal (Figure 4b, marked in purple) can be found at 16.7 ppm for **1b** (compare **I**: ^{29}Si = 16.10 ppm) and low-field shifted at 397 ppm for **1a**, which is within the typical range for acyclic silylenes (204–498 ppm).[3,7,11–13] That is in contrast to the previously reported **I**, whose room temperature NMR spectrum shows exclusively signals corresponding to the silepin. ^{1}H NMR analysis of the reaction mixture of **1a/b** also displays the presence of two species in a constant ratio of 2.7 : 1

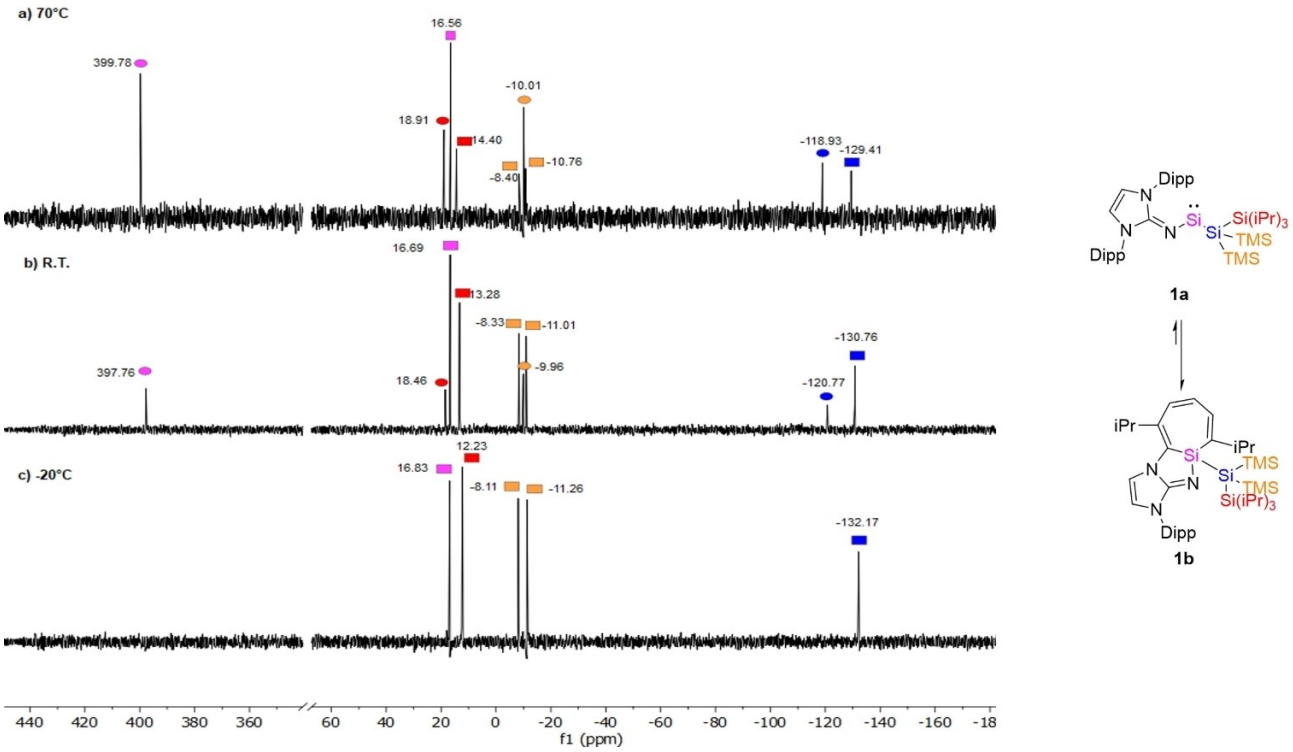

Figure 4. VT NMR measurement of **1a/b** in toluene-d8 (left), the spectra in the complete range and at further temperatures can be found in the Supporting Information: a) ^{29}Si NMR (80 MHz) spectrum at 70 °C, signals of **1a** marked as circles, signals of **1b** marked as squares b) ^{29}Si NMR (80 MHz) spectrum at room temperature, signals of **1a** marked as circles, signals of **1b** marked as squares; c) ^{29}Si NMR (80 MHz) spectrum at −20 °C, no observable signals of **1a**, signals of **1b** marked as squares. Colors of circles and squares correspond to the respective color of the silicon atom in the molecular structure (right).

(see Supporting Information). *Via* 2D NMR analysis a set of two TMS signals, and multiple doublets and multiplets belonging to the *iso*-propyl groups of the former Dipp-substituent and the $Si(^{i}Pr)_3$ group of the silyl ligand, could be assigned to the more prevalent, asymmetric silepin species **1 b**. Furthermore, a set of signals in the typical backbone range of NHC/NHI between 5.90 and 6.70 ppm could be assigned to the seven-membered silepin moiety and the former NHI backbone of **1 b**. A second set of one TMS signal, three doublets, a multiplet, and a signal set of the aromatic Dipp-group and the backbone of the NHI ligand can be assigned to the less prevalent silylene species **1 a**. The calculated ^{29}Si NMR spectroscopic shift of the central Si atom of **1 a** at 385.8 ppm is in good agreement with the experiment, further supporting the assignments. (For details regarding the computational studies see Supporting Information). The constant ratio between **1 a** and **1 b** at room temperature implies either a formation of a thermodynamic equilibrium between the two species, or a high isomerization barrier, not achievable at ambient conditions. Variable temperature (VT) NMR measurements at low and elevated temperatures were carried out to distinguish between the two scenarios. Decreasing the temperature of the reaction mixture results in a gradual decline of the NMR signals of **1 a** in the ^{1}H and ^{29}Si NMR spectra. The signals belonging to **1 a** completely disappear at $\approx -20\,^{\circ}C$ (Figure 4c), whereas the signals of **1 b** intensify. At the same time, a color change of the sample from green to yellow is observed. Reheating the sample to room temperature results in the reformation of **1 a** in the original ratio of **1 b**:**1 a** = 2.7:1 (calculated according to the ratio of TMS signals or NHI-backbone signals in the ^{1}H NMR spectrum) accompanied by reappearance of the intense green color.

Heating of the sample to 70 °C results in an opposite outcome. The ratio is continuously shifted towards the formation of **1 a**, whereas **1 b** declines until **1 a** becomes the dominant species (Figure 4a). Simultaneously, a color change from green to turquoise blue is observed.

These experiments suggest that **1 a** and **1 b** are in a thermodynamic equilibrium at ambient conditions. The equilibrium constant of K = 2.7 at room temperature derived from the NMR experiments corresponds to a Gibbs energy difference of 0.6 kcal mol^{-1} between **1 a** and **1 b** (at 298.15 K).

Further evidence for the equilibrium could be obtained from the respective VT UV/Vis measurements. At room temperature two maxima in the spectrum can be distinguished (Figure 5 a,b). An absorption band at 600 nm can be assigned to the "forbidden" n→3p transition of **1 a**, which was also observed in comparable compounds, *i.e.* the *N*-heterocyclic olefin-substituted silylene reported by Rivard[12] (583 nm) and the Cp*-substituted silylene reported by Leszczynska[5c] (530 nm). A similar absorption band was also observed for the previously reported silepin **I** at elevated temperatures (617 nm at 100°C). The second absorption band at 390 nm can partially be assigned to the silepin **1 b**, comparable to silepin **I** with an absorption band at 399 nm. TD-DFT calculations (Table S3, S4 and Figure S43, S44) show that the absorption in the visible region around 400 nm of **1 a** results from three charge transfer transitions with relatively high oscillator strength at 406.3, 376.3 and 372.3 nm (Figure 5d, red). The observed transition around 600 nm corresponds to the n→p excitation with a low oscillator strength and the calculated value of 588 nm. **1 b** shows only a single transition in the visible region, at 410.7 nm, resulting from the π→π* excitation (Figure 5d, blue). VT UV/Vis measure-

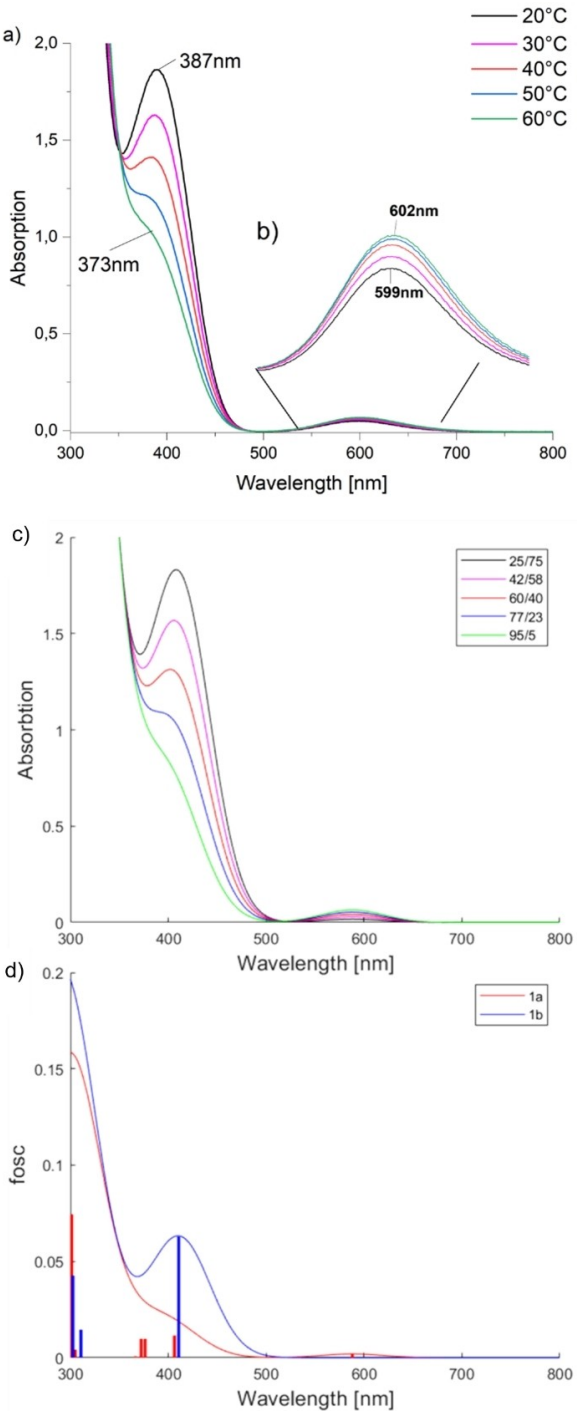

Figure 5. VT UV/Vis Measurement: a) whole spectrum at temperatures between 20 °C and 60 °C; b) close up on absorption band at 600 nm; c) Simulated spectrum of mixtures with **1 a**/**1 b** ratios of 25/75, 42/58, 60/40, 77/23, 95/5; d) Simulated spectra of **1 a** (red) and **1 b** (blue). The corresponding excitations are shown as vertical lines.

ments show that increasing the temperature to 60 °C leads to intensification of the absorption at 600 nm, which can be explained by the increase of the silylene isomer concentration at higher temperatures (Figure 5a,b). In contrast, the observable decay of the absorption maxima at 390 nm is attributed to the lower concentration of the silepin. The simulated UV/Vis spectrum of a mixture with different **1 a**/**1 b** ratios is presented in Figure 5c and reproduces well the experimental observations.

DFT calculations show that in **1 a** the intramolecular C–C bond insertion to form the silepin **1 b** is exergonic by only 1.2 kcal mol^{-1} at 298.15 K, which is in a very good agreement with the experimentally observed $\Delta G = -0.6$ kcal mol^{-1}.

In comparison, the intramolecular C–C bond insertion is calculated to be exergonic by 3.8 and 2.1 kcal mol^{-1} in the case of **I** and **J**, respectively. The differences are presumably caused by the steric bulk of the SiR_3 ligand. The largest ligand BTTPS makes the formation of the silepin isomer less favorable compared to **I** and **J**. In terms of the calculated enthalpy, **1 b** is favored by 2.8 kcal mol^{-1} in comparison to **1 a**, while in terms of Gibbs energy **1 b** is only favored by 1.2 kcal mol^{-1}. This is due to a larger entropy term of **1 a** (98.3 kcal mol^{-1} vs. 96.7 kcal mol^{-1} in **1 b** at 298.15 K). While the electronic, rotational, and translational entropy contributions are the same in both cases (0.0, 11.6, and 13.7 kcal mol^{-1}, respectively), the difference arises from the vibrational entropy term (73.1 kcal mol^{-1} in **1 a** and 71.4 kcal mol^{-1} in **1 b**). The larger entropy term should make **1 a** isomer more prevalent at elevated temperatures. This is in line with experimental observations showing a higher **1 a**/**1 b** ratio at higher temperatures.

The calculated potential energy surface (PES) for the proposed mechanism of the intramolecular C–C insertion in **1 a** is presented in Figure 6 (red) (details regarding the electronic structure of **1 a** are provided in the Computational Details section in the Supporting Information). For comparison, the reaction mechanisms for the previously reported **J'** and **I'** (Figure 6, green and blue) are also presented. The first step involves the reaction of the silylene across the aromatic C–C bond, dearomatizing the aryl and forming the Si(IV) norcaradiene type intermediates (**A**) at 7.6, 5.7, and 5.6 kcal mol^{-1}, respectively. The energies of the intermediates **A** relative to the starting compounds are distributed similarly to those of the silepins, indicating the role of the steric bulk of the SiR_3 substituent already at the first step of the process. At the second step, the single C–C bond of intermediate **A** is cleaved to form the silepin **1 b**, **J**, and **I** at −1.2, −2.1, and −3.8 kcal mol^{-1}. The reaction barriers for the forward and the reverse reactions in all of the compounds are relatively low (the highest barrier is **J** to **A-J** with $\Delta G^{\ddagger} = 17.6$ kcal mol^{-1}) and are achievable at room temperature, resulting in a silylene⇌silepin room temperature thermodynamic equilibrium. However, due to the energy differences between the reactants and the products, only in the case of **1 a/b** both the silylene and the silepin isomers can be observed at room temperature.

As we observed a facilitated conversion of the Si(IV) to the Si(II) species we were interested in the small molecule activation properties of **1 a/b**. The results are summarized in Scheme 2. When a degassed solution of compound **1 a/b** in toluene was treated with CO_2 gas at room temperature, the carboxylated product **2** was obtained. The compound exhibits a ^{13}C NMR shift of the carbonate carbon atom at 150.7 ppm, which is comparable to related literature known compounds (154.8–150.2 ppm).[6d,20] Mechanistic investigations of silylene carboxylation reactions have been conducted by Kira,[6c] we thus propose a similar reaction pathway. Another typical silylene reactivity was observed upon treatment of a degassed toluene

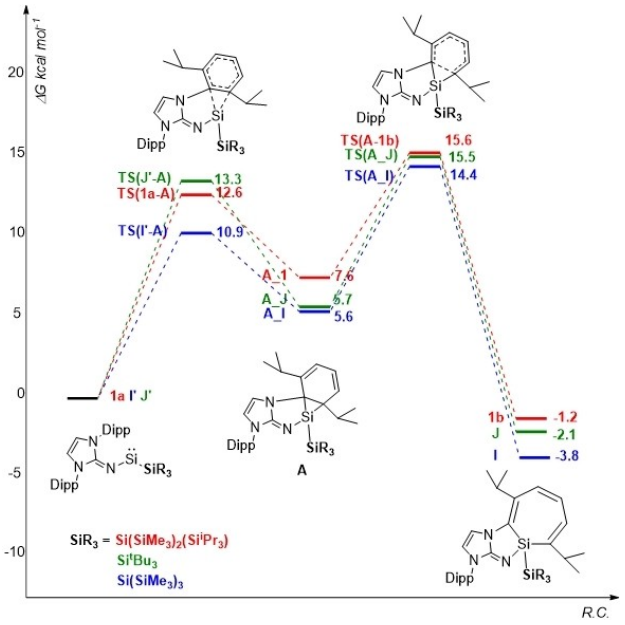

Figure 6. Calculated reaction pathway for the proposed mechanism of the intramolecular C–C insertion of silylenes **1 a**, **I** and **J.**

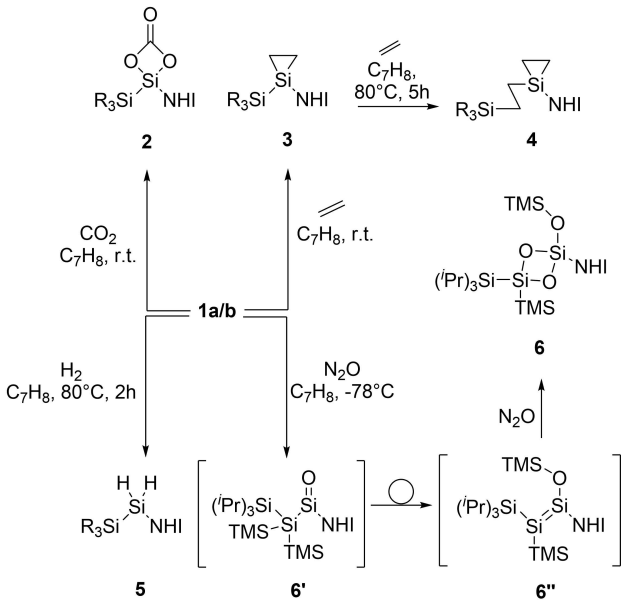

Scheme 2. Reactivity of compound **1 a/b** towards CO_2, ethylene, H_2 and N_2O. SiR_3 = BTTPS, NHI = bis(2,6- diisopropylphenyl)imidazoline-2-imine.

solution of **1 a/b** with ethylene at room temperature resulting in the formation of the silacyclopropane (silirane) **3**. Heating of **3** at 80 °C for five hours under ethylene atmosphere results in insertion of one molecule of ethylene into the Si–Si bond, forming the new silacyclopropane compound **4**, possibly induced by the release of steric strain caused by the large silyl substituent and the aryls of the NHI. Heating of an evacuated sample of **3** in toluene (without the presence of ethylene) to 100 °C for 16 h, leads to decomposition of **3** into a non-identifiable product mixture. Trace amounts of a reformed silylene / silepin (**1 a/b**) mixture can also be observed in the ^{1}H NMR spectrum.

Treatment of **1 a/b** in toluene with hydrogen gas and heating to 80 °C for two hours selectively affords the hydrogen addition product **5** with a $^{1}J_{Si\text{-}H}$ coupling constant of 187.8 Hz (compared to **I** with 189 Hz) corresponding to the silicon bound hydrogen atoms.

Thus, **1 a/b** seems to react in a similar fashion as the previously reported compounds **I** and **J** in the case of ethylene, hydrogen, and CO_2 with slightly enhanced reactivity towards hydrogen due to the smaller energy difference between the silylene and the silepin. In contrast, a deviation of reactivity towards N_2O was observed. While for literature known compounds either the formation of silanones or their dimers are a common outcome, in the case of **1 a/b** a fast and selective formation product **6** is achieved. In line with previous studies,[4b] we propose that the formation of **6** is initiated by the formation of silanone **6'**, followed by migration of a TMS from the BTTPS substituent to the oxygen atom, forming a transient disilene **6''**. A similar, but much slower migration process was also observed for the reaction of silepin **I** with N_2O. In this case, the respective silanone slowly decomposes in solution after migration of the TMS group but could be isolated in the presence of an NHC ligand. The enhancement of the formation of **6''** can be explained by the increased steric bulk at the central silicon atom of the BTTPS ligand, which results in a facilitation of the migration process. In the case of **1 a/b**, the fast second reaction of **6''** with a second equivalent of N_2O, forming the oxygen bridged compound **6** was achieved selectively. This represents a typical disilene reactivity, which was observable also in other cases, for example $[(TMS)_2N(\eta^1\text{-}Me_5C_5)Si{=}Si(\eta^1\text{-}Me_5C_5)N(TMS)_2]$ reported by Roesky and Stalke,[21] or the disilene $(Si^tBu_3)PhSi{=}SiPh(Si^tBu_3)$ reported by Wiberg.[22] Despite multiple attempts to trap the intermediates **6'** and **6''** with stoichiometric oxygen sources like $ONMe_3$, $NOBF_4$, (either no reaction or decomposition of the system) or by low temperature experiments (–78 °C), only the siloxy cyclodisiloxane **6** could be isolated due to its swift formation even at low temperatures.

The molecular structure of **6** was determined by SC-XRD analysis (Figure 7). The crystal structure shows two tetravalent silicon centers bridged by oxygen atoms. All Si–O bonds of the cyclodisiloxane moiety are nearly of similar length (1.671–1.699 Å) and are comparable to Roesky/Stalke's (1.67–1.68 Å)[21] and Wiberg's reported compounds (1.68-1.69 Å).[22] All angles of the cyclic unit are close to 90°. The same comparability can be observed for the Si1–Si2 atom distance of the cyclic silicon atoms of 2.401 Å.

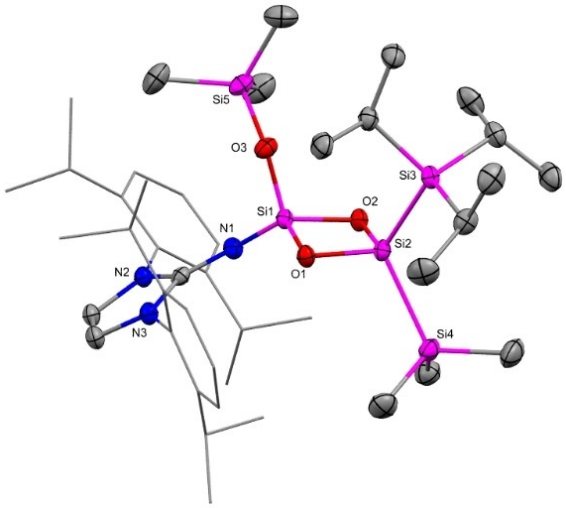

Figure 7. Molecular structure of **6**. Ellipsoids set at 50% probability; H atoms are omitted for clarity. Selected bond lengths [A] and angles [°]: Si1-O3 1.621(1), Si1-O2 1.678(1), Si2-O1 1.668(1), Si1-Si2 2.4014(8), Si1-N1 1.651(1), Si1-O2-Si2 91.26(5), O2-Si2-O1 89.44(5).

Conclusion

We synthesized a new acyclic silylene/silepin **1 a/b** with the sterically congested BTTPS ligand. The room-temperature-observable equilibrium, with 2.7 : 1 silepin/silylene ratio, was investigated by means of VT ^{29}Si NMR, VT ^{1}H NMR and VT UV/Vis measurement. Additionally, the conversion of the thermodynamically favored silepin to the silylene was investigated by DFT calculations. These results exemplify that facile oxidative addition/reductive elimination processes interconverting between Si(II) and Si(IV) at ambient conditions are achievable and provide insights into the prerequisites for controlling these processes. Compounds **1 a/b** demonstrate the significance of a substituent effect on the immanent reactivity. In this case, we observed facilitation of formation of the inherently more reactive Si(II) species. Due to the smaller energy difference between the silylene and silepin isomers, compared to the previously reported silepin **I**, **1 a/b** show enhanced silylene reactivity towards CO_2, ethylene, and H_2 to form the respective oxidative addition products. With ethylene, an additional insertion of one ethylene molecule into the Si–Si bond is possible resulting in the formation of the silirane **4**. Furthermore, **1 a/b** can undergo a double conversion of N_2O *via* formation of a transilient siloxy-substituted disilene to the corresponding siloxy-substituted cyclodisiloxane **6**. Further studies of related compounds concerning the Si(II)⇌Si(IV) interconversion and the enhanced reactivity facilitated by bulky substituents are underway. Potentially, these studies will enable us to develop additional reversible OA/RE processes, in which silicon can be established as the catalytically active metal center.

Experimental Section

Experimental procedures and relevant characterization data of newly synthesized compounds can be found in the Supporting Information along with DFT calculation details and XRD data. Deposition Number(s) 2192058 (for **1 b**), 2192059 (for **6**), contain(s) the supplementary crystallographic data for this paper. These data are provided free of charge by the joint Cambridge Crystallographic Data Centre and Fachinformationszentrum Karlsruhe Access Structures service.

Acknowledgements

We are exceptionally grateful to the WACKER Chemie AG for contributions in discussions and input and additionally for the idealistic and financial support, which enabled us to carry out this research project. We also thank Maximilian Muhr (Prof. R.A. Fischer) for conducting LIFDI-MS measurements and Theresa Bloehs for experimental support. The authors gratefully acknowledge the Leibniz Supercomputing Centre for funding this project by providing computing time on its Linux-Cluster. Open Access funding enabled and organized by Projekt DEAL.

Conflict of Interest

The authors declare no conflict of interest.

Data Availability Statement

The data that support the findings of this study are available in the supplementary material of this article.

Keywords: equilibrium · Si ligands · silylene · silepins · small molecule activation

[1] P. Jutzi, D. Kanne, C. Krüger, *Angew. Chem. Int. Ed. Engl.* **1986**, *25*, 164.
[2] a) S. Fujimori, S. Inoue, *Eur. J. Inorg. Chem.* **2020**, *2020*, 3131; b) C. Shan, S. Yao, M. Driess, *Chem. Soc. Rev.* **2020**, *49*, 6733.
[3] A. V. Protchenko, K. H. Birjkumar, D. Dange, A. D. Schwarz, D. Vidovic, C. Jones, N. Kaltsoyannis, P. Mountford, S. Aldridge, *J. Am. Chem. Soc.* **2012**, *134*, 6500.
[4] a) A. C. Filippou, B. Baars, O. Chernov, Y. N. Lebedev, G. Schnakenburg, *Angew. Chem. Int. Ed.* **2014**, *53*, 565; b) D. Wendel, D. Reiter, A. Porzelt, P. J. Altmann, S. Inoue, B. Rieger, *J. Am. Chem. Soc.* **2017**, *139*, 17193; c) I. Alvarado-Beltran, A. Rosas-Sánchez, A. Baceiredo, N. Saffon-Merceron, V. Branchadell, T. Kato, *Angew. Chem. Int. Ed.* **2017**, *56*, 10481; d) A. Rosas-Sánchez, I. Alvarado-Beltran, A. Baceiredo, N. Saffon-Merceron, S. Massou, D. Hashizume, V. Branchadell, T. Kato, *Angew. Chem. Int. Ed.* **2017**, *56*, 15916.
[5] a) R. Holzner, D. Reiter, P. Frisch, S. Inoue, *RSC Adv.* **2020**, *10*, 3402; b) J. Keuter, A. Hepp, F. Lips, *Eur. J. Org. Chem.* **2022**, *2022*, e202101238; c) K. I. Leszczyńska, P. Deglmann, C. Präsang, V. Huch, M. Zimmer, D. Schweinfurth, D. Scheschkewitz, *Dalton Trans.* **2020**, *49*, 13218; d) D. Wendel, W. Eisenreich, C. Jandl, A. Pöthig, B. Rieger, *Organometallics* **2016**, *35*, 1.
[6] a) D. Gau, R. Rodriguez, T. Kato, N. Saffon-Merceron, A. de Cózar, F. P. Cossío, A. Baceiredo, *Angew. Chem. Int. Ed.* **2011**, *50*, 1092; b) P. Jutzi, D. Eikenberg, A. Möhrke, B. Neumann, H.-G. Stammler, *Organometallics* **1996**, *15*, 753; c) X. Liu, X.-Q. Xiao, Z. Xu, X. Yang, Z. Li, Z. Dong, C. Yan, G. Lai, M. Kira, *Organometallics* **2014**, *33*, 5434; d) R. Rodriguez, I. Alvarado-Beltran, J. Saouli, N. Saffon-Merceron, A. Baceiredo, V. Branchadell, T. Kato, *Angew. Chem. Int. Ed.* **2018**, *57*, 2635.
[7] B. D. Rekken, T. M. Brown, J. C. Fettinger, H. M. Tuononen, P. P. Power, *J. Am. Chem. Soc.* **2012**, *134*, 6504.
[8] B. D. Rekken, T. M. Brown, J. C. Fettinger, F. Lips, H. M. Tuononen, R. H. Herber, P. P. Power, *J. Am. Chem. Soc.* **2013**, *135*, 10134.
[9] Y. K. Loh, L. Ying, M. Ángeles Fuentes, D. C. H. Do, S. Aldridge, *Angew. Chem. Int. Ed.* **2019**, *58*, 4847.
[10] D. Reiter, P. Frisch, D. Wendel, F. M. Hörmann, S. Inoue, *Dalton Trans.* **2020**, *49*, 7060.
[11] a) A. V. Protchenko, A. D. Schwarz, M. P. Blake, C. Jones, N. Kaltsoyannis, P. Mountford, S. Aldridge, *Angew. Chem. Int. Ed.* **2013**, *52*, 568; b) T. J. Hadlington, J. A. B. Abdalla, R. Tirfoin, S. Aldridge, C. Jones, *Chem. Commun.* **2016**, *52*, 1717.
[12] M. M. D. Roy, M. J. Ferguson, R. McDonald, Y. Zhou, E. Rivard, *Chem. Sci.* **2019**, *10*, 6476.
[13] D. Wendel, A. Porzelt, F. A. D. Herz, D. Sarkar, C. Jandl, S. Inoue, B. Rieger, *J. Am. Chem. Soc.* **2017**, *139*, 8134.
[14] H. Sohn, J. Merritt, D. R. Powell, R. West, *Organometallics* **1997**, *16*, 5133.
[15] J. Y. Corey, M. Dueber, B. Bichlmeir, *J. Organomet. Chem.* **1971**, *26*, 167.
[16] Y. Nakadaira, R. Sato, H. Sakurai, *Organometallics* **1991**, *10*, 435.
[17] a) T. Kosai, S. Ishida, T. Iwamoto, *Chem. Commun.* **2015**, *51*, 10707–10709; b) T. Kosai, S. Ishida, T. Iwamoto, *Angew. Chem. Int. Ed.* **2016**, *55*, 15554.
[18] a) H. Suzuki, N. Tokitoh, R. Okazaki, *J. Am. Chem. Soc.* **1994**, *116*, 11572; b) H. Suzuki, N. Tokitoh, R. Okazaki, *Bull. Chem. Soc. Jpn.* **1995**, *68*, 2471.
[19] L. Zhu, J. Zhang, C. Cui, *Inorg. Chem.* **2019**, *58*, 12007.
[20] M. Denk, R. Lennon, R. Hayashi, R. West, A. V. Belyakov, H. P. Verne, A. Haaland, M. Wagner, N. Metzler, *J. Am. Chem. Soc.* **1994**, *116*, 2691.
[21] S. Khan, R. Michel, D. Koley, H. W. Roesky, D. Stalke, *Inorg. Chem.* **2011**, *50*, 10878.
[22] N. Wiberg, W. Niedermayer, K. Polborn, P. Mayer, *Chem. Eur. J.* **2002**, *8*, 2730.

Manuscript received: July 26, 2022
Accepted manuscript online: September 13, 2022
Version of record online: October 19, 2022